Stretchable, Transparent, Ionic Conductors

Christoph Keplinger,[1,2,3]* Jeong-Yun Sun,[1,2]* Choon Chiang Foo,[1,2,4] Philipp Rothemund,[1,2] George M. Whitesides,[2,3,5]† Zhigang Suo[1,2]†

Existing stretchable, transparent conductors are mostly electronic conductors. They limit the performance of interconnects, sensors, and actuators as components of stretchable electronics and soft machines. We describe a class of devices enabled by ionic conductors that are highly stretchable, fully transparent to light of all colors, and capable of operation at frequencies beyond 10 kilohertz and voltages above 10 kilovolts. We demonstrate a transparent actuator that can generate large strains and a transparent loudspeaker that produces sound over the entire audible range. The electromechanical transduction is achieved without electrochemical reaction. The ionic conductors have higher resistivity than many electronic conductors; however, when large stretchability and high transmittance are required, the ionic conductors have lower sheet resistance than all existing electronic conductors.

The emergence of the field of stretchable electronics, along with its biomedical applications, has highlighted a challenge: Electronic devices are usually made of hard materials, whereas tissues and cells are soft. Stretchable conductors are needed to enable electronics to meet skin, heart, and brain (*1*, *2*). Stretchable conductors are also needed in applications, such as electromechanical transduction (*3*) and solar energy conversion (*4*). Existing stretchable conductors are mostly electronic conductors, including carbon grease (*5*), microcracked gold films (*6*), serpentine-shaped metallic wires (*1*), carbon nanotubes (*7*, *8*), graphene sheets (*9*, *10*), and silver nanowires (*11*–*13*). Stretchable devices have also been made by using corona discharge (*14*), liquid metals (*15*), and saline solutions (*16*); these conductors, however, are not solid, and their uses are limited. Attributes other than conductivity and stretchability are also important in specific applications. Conductors may need to operate at high frequencies and high voltages (*5*), remain conductive while undergoing areal expansions of 1000% or more (*17*), be biocompatible (*3*), and be transparent (*7*–*13*).

Whereas electronic conductors struggle to meet these demands, ionic conductors meet most of them readily. Many ionic conductors, such as hydrogels (*18*) and gels swollen with ionic liquids (*19*), take a solid form and are stretchable and transparent. Many hydrogels are biocompatible and conformal to tissues and cells down to the molecular scale (*20*). We demonstrate that ionic conductors can even be used in devices requiring voltages and frequencies much higher than those commonly associated with devices using ionic conductors.

One basic design places two electrodes (electronic conductors), an electrolyte (ionic conductor), and a dielectric (insulator) in series (Fig. 1A). The electrode/electrolyte interface forms an electrical double layer (Fig. 1B). For some combinations of the electrode and electrolyte, if the voltage across the interface is within a certain range (~1 V), the interface is ideally polarizable—that is, electrons and ions do not cross the interface, no electrochemical reaction occurs, and the electrical double layer behaves like a capacitor (Fig. 1C). A circuit with electronic and ionic conductors in series cannot carry sustained electrical current in the absence of electrochemical reaction. The electrical double layer and the dielectric are two capacitors in series. They capacitively couple the electrical signals carried by the two electrodes and transport power with alternating current.

The two capacitors have vastly different capacitances. For the electrical double layer, charges in the electrode and in the electrolyte are separated over nanometers; this small separation leads to a large capacitance, on the order of $c_{EDL} \sim 10^{-1}$ F/m^2 (*19*). For the dielectric, charges on its two faces are separated over the thickness of the dielectric (millimeters in our experiments); this large separation leads to a small capacitance, on the order of $c_D \sim 10^{-8}$ F/m^2. At equilibrium, the voltage V applied between the two electrodes is carried entirely by the electrical double layer and the dielectric, $V = V_{EDL} + V_D$ (Fig. 1A). In response to the applied voltage, the two capacitors add the same amount of charge, $c_D A_D V_D = c_{EDL} A_{EDL} V_{EDL}$, where A_{EDL} is the area of the electrical double layer and A_D is the area of the dielectric. In our experiments, $A_{EDL}/A_D \sim 0.01$; the large ratio $c_{EDL}/c_D \sim 10^7$ ensures that the voltage across the electrical double layer V_{EDL} is well below 1 V when the voltage across the dielectric is on the order of $V_D \sim 10$ kV. A small V_{EDL} prevents electrochemical reaction, whereas a large V_D enables electromechanical transduction.

We built a transparent, high-speed, large-strain actuator. A membrane of a dielectric elastomer was sandwiched between two membranes of an electrolytic elastomer (Fig. 2A and fig. S1). The dielectric and the electrolyte are stretchable and transparent, but the electrodes need not be. The electrode/electrolyte interfaces can be much smaller than the area of the dielectric, allowing us to place

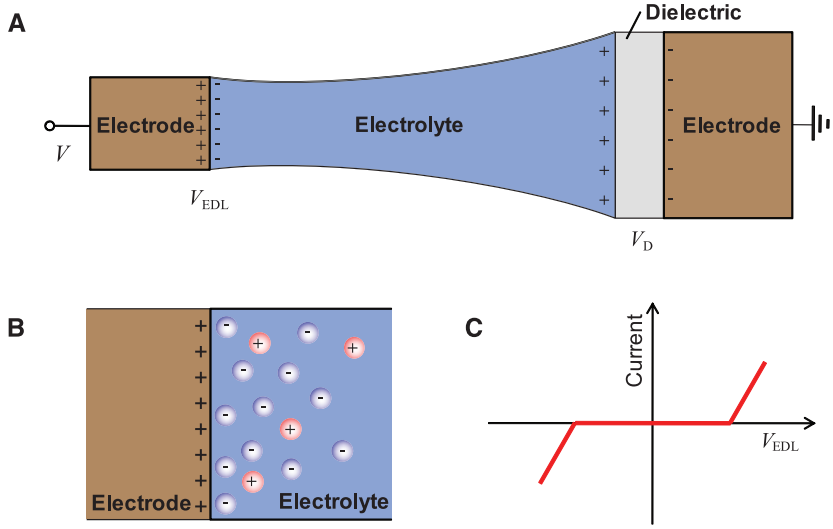

Fig. 1. A basic design of stretchable ionics. (**A**) An electrolyte and a dielectric are in series. When they are elastomeric, the device is solid and stretchable. When a voltage V is applied between the two electrodes, the voltage across the electrode/electrolyte interface is much smaller than the voltage across the dielectric, $V_{EDL} \ll V_D$. (**B**) The electrode/electrolyte interface forms an electrical double layer. (**C**) When the voltage across the interface is within a certain range, electrons and ions do not cross the interface, no electrochemical reaction occurs, and the electrical double layer behaves like a capacitor.

[1]School of Engineering and Applied Sciences, Harvard University, Cambridge, MA 02138, USA. [2]Kavli Institute for Bionano Science and Technology, Harvard University, Cambridge MA 02138, USA. [3]Department of Chemistry and Chemical Biology, Harvard University, Cambridge, MA 02138, USA. [4]Institute of High Performance Computing, 1 Fusionopolis Way, 138632 Singapore. [5]Wyss Institute for Biologically Inspired Engineering, Harvard University, Cambridge MA 02138, USA.

*These authors contributed equally to this work.
†Corresponding author. E-mail: GWhitesides@gmwgroup.harvard.edu (G.M.W.); suo@seas.harvard.edu (Z.S.)

the electrodes outside the active region. Consequently, the active region of the actuator consisted of only electrolytic and dielectric elastomers and was highly stretchable and transparent. When a voltage was applied between the electrodes, ions of different charge polarities collected on the two faces of the dielectric; the oppositely charged interfaces attracted each other and caused the sandwich to reduce its thickness and enlarge its area (Fig. 2B).

We demonstrated this design by using 1-mm-thick VHB 4910 tape (3M) as the dielectric and 100-μm-thick polyacrylamide hydrogel containing NaCl as the electrolyte. To compare the performance of the ionic conductor to an electronic conductor, we used the hydrogel to replace the carbon grease in the actuator used in (*5*). We stacked three layers of VHB together, stretched them radially to three times their initial radius, and fixed them to a circular acrylic frame (fig. S1). We then sandwiched the dielectric stack between two layers of heart-shaped hydrogels, which are linked, through thin hydrogel lines, to copper electrodes placed on the frame. When a voltage is applied and removed, the heart expands and contracts (movie S1). The beating heart is transparent to all colors (Fig. 2, C and D).

We also fabricated an actuator with the dielectric sandwiched between layers of the hydrogels of circular shape and compared the experimental data with theory (fig. S2). An area strain of up to 167% was achieved (Fig. 2, E and F). This voltage-induced strain was limited by electromechanical instability (fig. S3). Furthermore, the soft hydrogels did not appreciably constrain the dielectric. The area strain of our actuator reduced as the frequency of applied voltage increased and became vanishingly small at a frequency on the order of 10^3 Hz (Fig. 2F). These characteristics of the actuator using the hydrogel are comparable to those of an actuator using carbon grease (fig. S4), but the carbon grease is an opaque electronic conductor.

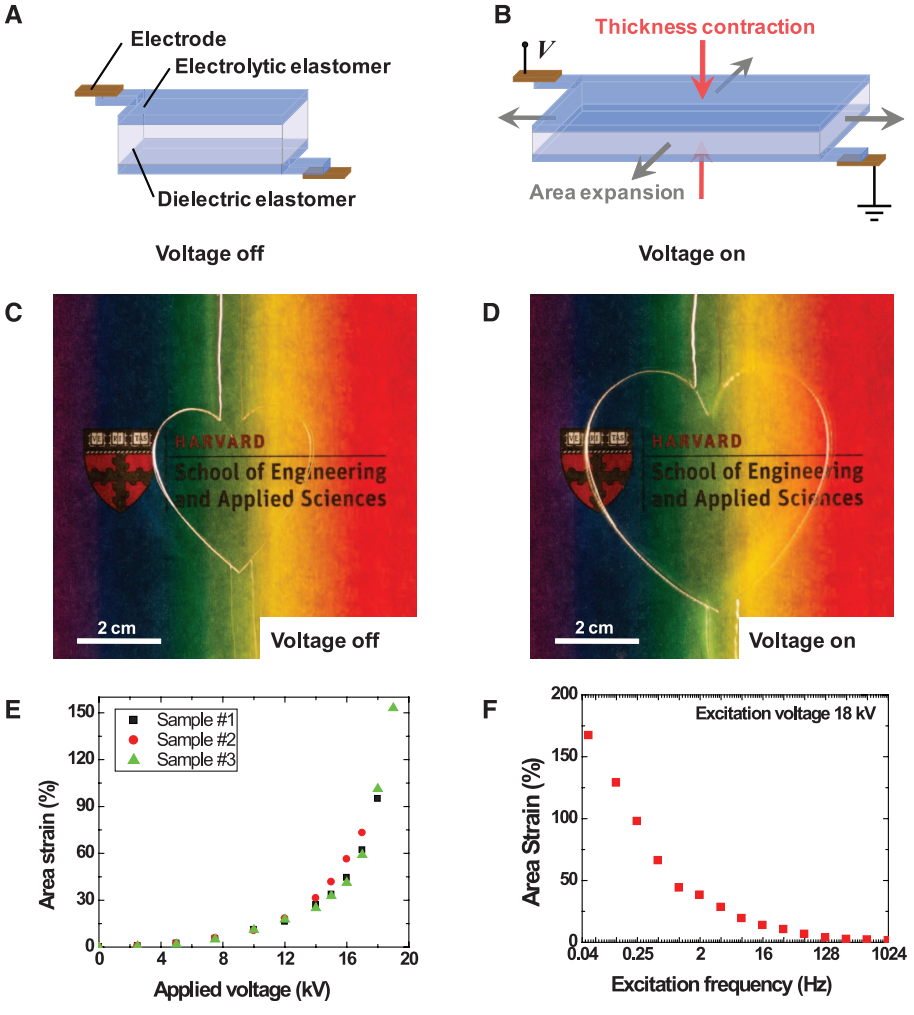

Fig. 2. Transparent actuator capable of fast voltage-induced deformation. (**A**) A dielectric elastomer is sandwiched between two layers of an electrolytic elastomer. Both the dielectric and the electrolyte are transparent and stretchable, and the device is transparent if the electrodes are placed outside the active area of the device. (**B**) Subject to voltage, the two layers of the electrolyte spread ions of opposite signs on the two sides of the dielectric, causing the sandwich to reduce thickness and expand area. (**C** and **D**) The actuator is transparent to all colors. The area strain is measured as a function of voltage (**E**) and as a function of the frequency (**F**) by using an actuator with electrolytes of circular shape.

The frequency of actuation is not limited by electrical resistance but by mechanical inertia. The time to charge the device, the RC delay, scales as $\tau_{RC} \sim c_D A_D R$, where R is the sheet resistance of the ionic conductor. For representative values $c_D = 10^{-8}$ F/m^2, $A_D = 10^{-2}$ m^2, and $R = 10^2$ ohm/square, we estimate that $\tau_{RC} \sim 10^{-8}$ s, corresponding to a frequency much higher than the observed limiting frequency of actuation. The fundamental resonance sets a time $\tau_{inertia} \sim \sqrt{A_D \rho / Y}$, where ρ is the mass density and Y the elastic modulus. For representative values $\rho = 10^3$ kg/m^3 and $Y = 10^5$ N/m^2, we estimate that $\tau_{inertia} \sim 10^{-3}$ s; this value is consistent with the observed limiting frequency of actuation.

To demonstrate that the ionic conductors enable electromechanical transduction much beyond the fundamental resonance, we built a transparent loudspeaker that produces sound across the entire audible range, from 20 Hz to 20 kHz. The loudspeaker was placed in front of a laptop, which played music videos (Fig. 3, A and B, and fig. S5). The screen of the laptop was visible through the loudspeaker. The sound tracks of the videos were fed to the loudspeaker as analog voltage signals, from the audio output of the laptop, through a high-voltage amplifier. A video of the transparent loudspeaker and the sound produced were recorded with a Web camera (webcam) at a distance of 15 cm (movie S2).

We studied the fidelity of the sound reproduction by feeding the loudspeaker with a 20-s test signal of constant amplitude and a linear sine sweep from 20 Hz to 20 kHz (Fig. 3, C and D). The sound generated by the loudspeaker was recorded by the webcam (movie S3). In the first few seconds, the amplitude of the recorded sound was large (Fig. 3E). This interval reflects the resonance of the frame of the loudspeaker, which was not optimized to suppress vibration. The amplitude varied only slightly over the remainder of the recording, where variations in amplitude might be overshadowed by background noise from the high-voltage amplifier. The spectrogram of the recorded sound displayed the successful reproduction of the main signal of the original test sound throughout the audible frequency range (Fig. 3F). In the lower part of the tested frequency range, vibrations of the frame and the membrane were visible (movie S4).

Loudspeakers have been made by using electronic conductors, such as graphene sheets (*21*), carbon nanotubes (*22*), carbon grease (*23*), and conducting polymers (*24*). Some loudspeakers use piezoelectric polymers (*21*, *22*), and others use dielectric elastomers (*23*, *24*). Pairing the ionic conductors with transparent piezoelectric polymers will take advantage of the high transparency of the ionic conductors; piezoelectric polymers can be operated with lower electric

fields compared with dielectric elastomers and have a linear relation between electric field and strain (*21*, *22*).

The ionic conductors have higher resistivity than many electronic conductors; however, when high stretchability and transmittance are required, the ionic conductors have lower sheet resistance than existing electronic conductors, such as silver nanowires (AgNWs), single-wall carbon nanotubes (SWNTs), graphene, and indium tin oxide (ITO). The resistivity of the hydrogel is almost identical to that of water containing the same concentration of NaCl when the hydrogel is not stretched and increases when the hydrogel is stretched (Fig. 4A). For a conductor whose resistivity is independent of deformation, the resistance of the conductor increases with stretch as $R/R_0 = \lambda^2$, where R_0 is the resistance before the conductor is stretched and R is the resistance after the conductor is stretched λ times its initial length. This prediction closely approximates the measured resistance-stretch curve for the ionic hydrogel (Fig. 4B). When SWNTs on VHB are stretched, the resistance increases far faster than the prediction of the square law, indicating that the resistivity of the SWNTs is increased greatly by the stretch. An 11-mm-thick hydrogel containing 5.48 M NaCl shows 98.9% average transmittance in the visible range (Fig. 4C), corresponding to a transmittance of 99.99% for a 100-μm-thick hydrogel used in constructing actuators and loudspeakers. Among all conductors of electricity, these hydrogels show the highest transmittance (Fig. 4D).

The diversity of ionic conductors creates a large pool of candidates for applications. Hydrogels are easy to make and inexpensive, ideal for demonstrating conceptual designs and for fabricating devices that require biocompatibility. In higher organisms, it is ionic conductors that transmit in vivo information. This characteristic offers the potential to build nondamaging interfaces between ionic/biological and ionic/electronic signals. Although the loss of water from hydrogels can be an issue in some applications, the rate of evaporation may be reduced by encapsulation. Also, ionic liquids are nonvolatile electrolytes and can be used as conductors for large-strain, high-speed dielec-

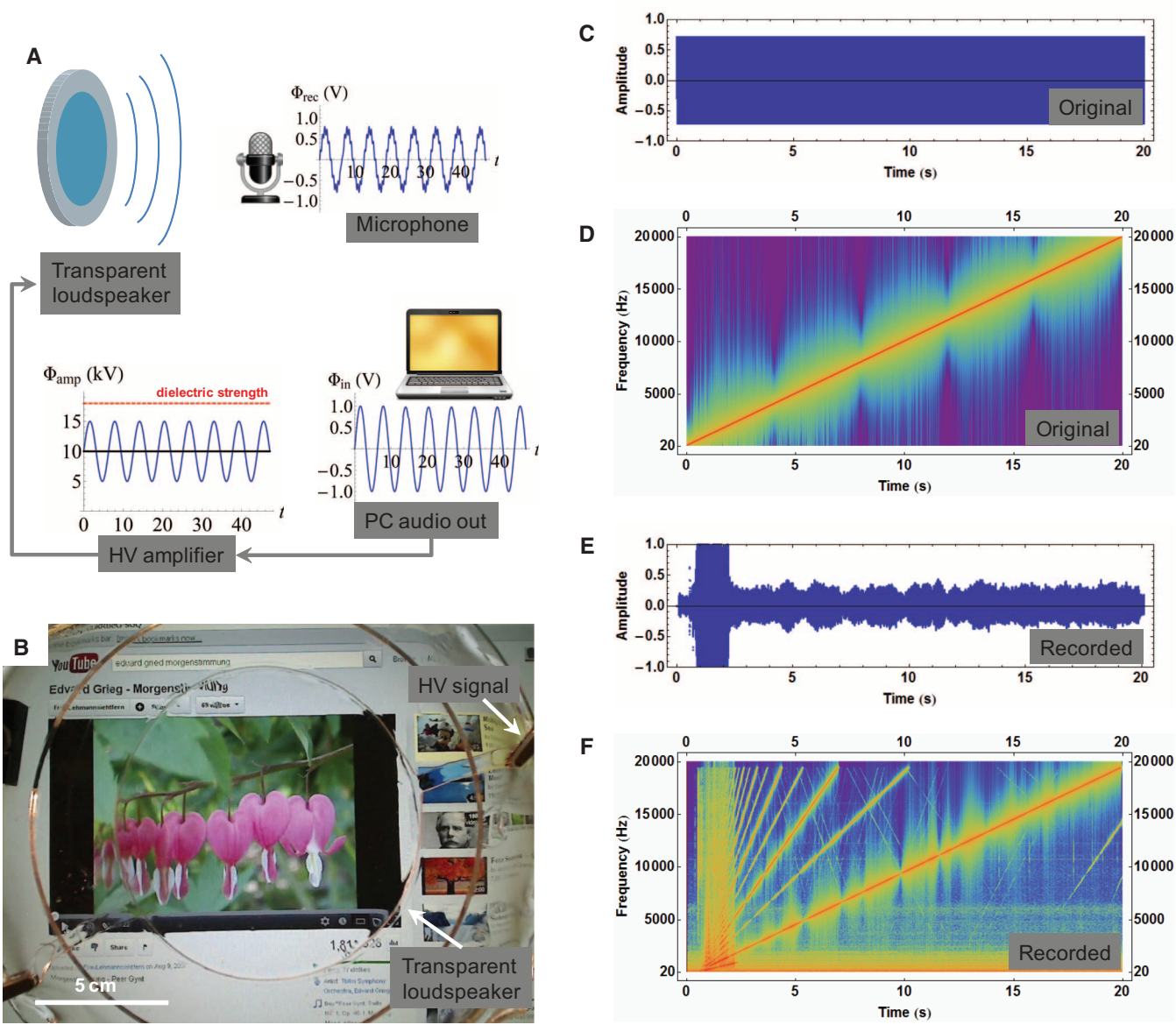

Fig. 3. Transparent loudspeaker capable of producing sound across the entire audible range. (**A**) The voltage signal from the audio output of a laptop was fed through a high-voltage amplifier to the loudspeaker. The loudspeaker transformed the voltage signal into sound, which was recorded with a microphone. (**B**) The screen of the laptop was visible through the loudspeaker. Amplitude (**C**) and spectrogram (**D**) of a test signal with constant amplitude and a linear sine sweep of frequency from 20 Hz to 20 kHz. The colors correspond to the intensities of frequency, with warmer colors indicating higher intensity. Amplitude (**E**) and spectrogram (**F**) of the sound generated by the loudspeaker.

tric elastomer actuators (fig. S6). Furthermore, it will be interesting to explore polyelectrolytes, in which charged polymers covalently cross-link into networks, and counterions are mobile.

Replacing electronic conductors with ionic conductors raises further scientific questions. For example, various types of conductors may lead to different characteristics of charge transport through the dielectric. We have measured charge leakage through VHB when three types of conductors are used: carbon grease, a hydrogel, and an ionic liquid. The three types of conductors give a comparable time scale for leakage for the chosen experimental conditions (fig. S7). As a second example, we used thin lines of ionic conductors, hydrogels and ionic liquids, to link active regions of devices to the copper electrodes. Our calculations indicate that ionic conductors can serve as high-speed, long-distance interconnects (fig. S8). As a third example, the lifetime of a device depends on the electrolyte, the dielectric, and the electrode. However, finding ideal combinations of materials for long lifetimes is a large undertaking beyond the scope of this paper.

Our design of layered electrolytic and dielectric elastomers differs from existing transducers in which ionic conduction plays essential roles, such as actuators made of carbon nanotubes and conducting polymers in electrolytes (*25*, *26*), actuators made of ionic polymer–metal composites (*27*), and resistive strain sensors made of elastomeric ionic hydrogels (*28*). Our design introduces a dielectric in series with an electrolyte, and the small capacitance of the dielectric enables high-speed and large-strain actuation. Layered electrolytes and dielectrics also appear in one set of electrowetting devices, but the electrolytes are liquids, and the dielectrics do not deform (*29*).

Stretchable ionics offer new opportunities for designers of soft machines. Dielectric elastomers have been paired with electronic conductors to make transducers in robotics, bioelectronics, and energy harvesting (*30*). Pairing dielectric elastomers with ionic conductors will substantially expand the scope of applications, leading to devices such as tunable optics and localized haptics with transparent ionic conductors placed in the path of the light. Transparent loudspeakers might be attached to windows to achieve active noise cancellation (*22*). The ultrahigh transparency and compliance of the ionic conductors will enable transparent devices of multilayered electrolytic and dielectric elastomers. To scale up the active area of a device, one can enlarge the electrode/electrolyte interface by using porous electrodes, such as those used in supercapacitors. This paper focuses on the use of ionic conductors in devices operating at high speed and under high voltage, but the layered electrolytic and dielectric elastomer also works for applications that require low voltage or low frequency. When stretched mechanically, the layered material increases area and reduces thickness, so that its capacitance increases. This characteristic will enable transparent sensors operating at low voltage, capable of measuring strains over a large range, and conformal to soft tissues.

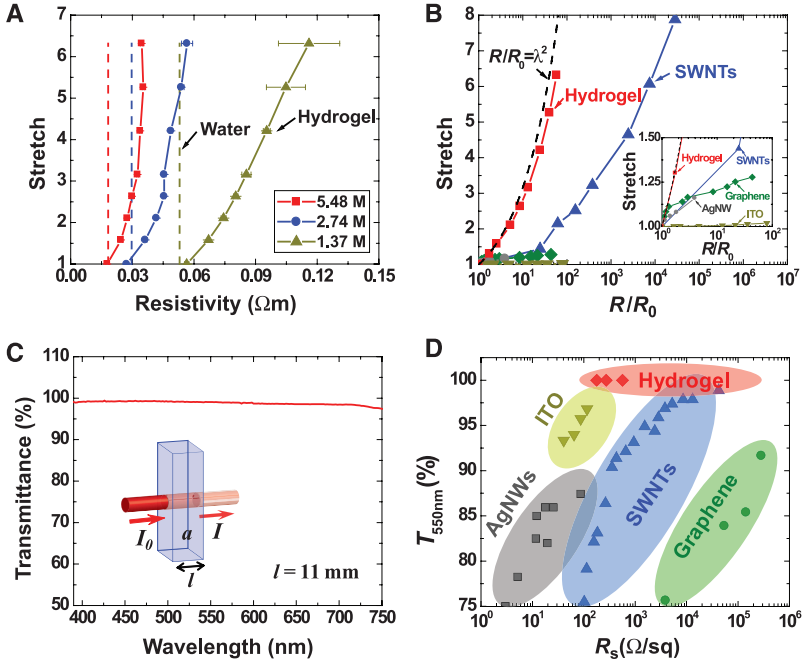

Fig. 4. Performance of ionic and electronic conductors. (**A**) Electrical resistivities of hydrogels of several concentrations of NaCl were measured as functions of stretch and compared with the resistivities of water containing the same concentrations of NaCl. Error bars show standard deviation; sample size $N = 3$. (**B**) Stretch was plotted against normalized resistance for ITO (*13*), AgNWs (*12*), graphene (*9*), SWNTs (*7*), and hydrogel (this work). (Inset) Details in the small stretch region. (**C**) An 11-mm-thick polyacrylamide hydrogel containing 5.48 M NaCl shows 98.9% average transmittance in the visible range. (**D**) Transmittance (at 550 nm) is plotted against sheet resistance for ITO (*12*), AgNWs (*11*), SWNTs (*8*), graphene (*10*), and hydrogels (100-μm thickness, this work).

References and Notes

1. D.-H. Kim *et al.*, *Science* **333**, 838–843 (2011).
2. T. Someya, Ed., *Stretchable Electronics* (Wiley-VCH, Weinheim, Germany, 2013).
3. S. Rosset, H. R. Shea, *Appl. Phys. A Mater. Sci. Process.* **110**, 281–307 (2013).
4. D. J. Lipomi, Z. Bao, *Energy Environ. Sci.* **4**, 3314–3328 (2011).
5. R. Pelrine, R. Kornbluh, Q. Pei, J. Joseph, *Science* **287**, 836–839 (2000).
6. S. P. Lacour, S. Wagner, Z. Huang, Z. Suo, *Appl. Phys. Lett.* **82**, 2404–2406 (2003).
7. L. Hu, W. Yuan, P. Brochu, G. Gruner, Q. Pei, *Appl. Phys. Lett.* **94**, 161108 (2009).
8. V. Scardaci, R. Coull, J. N. Coleman, *Appl. Phys. Lett.* **97**, 023114 (2010).
9. K. S. Kim *et al.*, *Nature* **457**, 706–710 (2009).
10. S. De *et al.*, *Small* **6**, 458–464 (2010).
11. S. De *et al.*, *ACS Nano* **3**, 1767–1774 (2009).
12. Z. Yu *et al.*, *Adv. Mater.* **23**, 664–668 (2011).
13. W. Hu *et al.*, *Nanotechnology* **23**, 344002 (2012).
14. C. Keplinger, M. Kaltenbrunner, N. Arnold, S. Bauer, *Proc. Natl. Acad. Sci. U.S.A.* **107**, 4505–4510 (2010).
15. M. D. Dickey *et al.*, *Adv. Funct. Mater.* **18**, 1097–1104 (2008).
16. Q. Zhao *et al.*, *Appl. Phys. Lett.* **100**, 101902 (2012).
17. C. Keplinger, T. Li, R. Baumgartner, Z. Suo, S. Bauer, *Soft Matter* **8**, 285–288 (2012).
18. J. Y. Sun *et al.*, *Nature* **489**, 133–136 (2012).
19. K. H. Lee *et al.*, *Adv. Mater.* **24**, 4457–4462 (2012).
20. K. Y. Lee, D. J. Mooney, *Chem. Rev.* **101**, 1869–1880 (2001).
21. S. C. Xu *et al.*, *Appl. Phys. Lett.* **102**, 151902 (2013).
22. X. Yu, R. Rajamani, K. A. Stelson, T. Cui, *Sens. Actuators A Phys.* **132**, 626–631 (2006).
23. R. Heydt, R. Kornbluh, J. Eckerle, R. Pelrine, *Proc. SPIE* **6168**, 61681M1–61681M8 (2006).
24. T. Sugimoto *et al.*, *J. Acoust. Soc. Am.* **130**, 744–752 (2011).
25. R. H. Baughman *et al.*, *Science* **284**, 1340–1344 (1999).
26. E. W. H. Jager, E. Smela, O. Inganäs, *Science* **290**, 1540–1545 (2000).
27. M. Shahinpoor, Y. Bar-Cohen, J. O. Simpson, J. Smith, *Smart Mater. Struct.* **7**, R15–R30 (1998).
28. P. Manandhar, P. D. Calvert, J. R. Buck, *IEEE Sens. J.* **12**, 2052–2061 (2012).
29. C. Quilliet, B. Berge, *Curr. Opin. Colloid Interface Sci.* **6**, 34–39 (2001).
30. F. Carpi, S. Bauer, D. De Rossi, *Science* **330**, 1759–1761 (2010).

Acknowledgments: This work is supported by the NSF Materials Research Science and Engineering Centers (DMR-0820484) and by the Army Research Office (W911NF-09-1-0476). We acknowledge Department of Energy award number ER45852 for salary support of C.K.; C.C.F. acknowledges support from A*STAR graduate scholarship (Post-Doctoral Fellowship). The authors (J.-Y.S., C.K., Z.S., and G.M.W.) have filed a patent application relating to stretchable, ionic, ultratransparent conductors capable of operation at high frequency and voltage. We acknowledge the discussions with D. Bwambok and H. Ardebili and her students on ionic liquids.

Supplementary Materials

www.sciencemag.org/cgi/content/full/341/6149/984/DC1
Materials and Methods
Supplementary Text
Figs. S1 to S8
References (*31*–*43*)
Movies S1 to S4

8 May 2013; accepted 22 July 2013
10.1126/science.1240228